metals

MDPI

Article

A Simple, Reusable and Low-Cost LVDT-Based in Situ Bolt Preload Monitoring System during Fastening for a Truck Wheel Assembly

Shin Jang †, Juhyun Nam †, Samgon Lee and Je Hoon Oh *

Department of Mechanical Engineering, Hanyang University, 55 Hanyangdaehak-ro, Sangrok-gu, Ansan, Gyeonggi-do 15588, Korea; maestro409@gmail.com (S.J.); jhnam10@hanyang.ac.kr (J.N.); tee5teen@hanyang.ac.kr (S.L.)

* Correspondence: jehoon@hanyang.ac.kr; Tel.: +82-31-400-5252

† These authors contributed equally to this work.

Received: 11 February 2019; Accepted: 12 March 2019; Published: 16 March 2019

Abstract: The aim of this study is to design and test a new, simple, and reusable linear variable differential transformer (LVDT)-based in situ bolt preload monitoring system (L-PMS) during fastening of a truck wheel assembly. Instead of measuring the elongation of a bolt, the distance between the end surfaces of both the bolt and nut was monitored via the L-PMS. The distance obtained from the L-PMS was experimentally correlated with the actual preload measured by a washer-type load cell. Since the variation of the distance is related to the stiffness of the bolt and clamped parts, a finite element analysis was also conducted to predict the sensitivity of L-PMS. There was a strong linear relationship between the distance and bolt preload after the bolt and nut were fully snugged. However, a logarithm-shaped nonlinear relationship was irregularly observed before getting snugged, making it difficult to define a clear relationship. In order to tackle this issue, an arc-shaped conductive line was screen-printed onto the surface of the clamped parts using a conductive carbon paste. The results show that a resistance variation of the conductive line during fastening enables to determine the snug point, so the L-PMS combined with resistance measurement results in an approximately ±6% error in the measurement of bolt preload. The proposed L-PMS offers a simple but highly reliable way for measuring bolt preload during fastening, which could be utilized in a heavy-truck production line.

Keywords: bolted joint; bolt preload; preload monitoring; resistance change; snug point; truck wheel

1. Introduction

Bolts have been widely used for assembling machine components owing to the associated easy-tightening process and their relative insensitivity to service temperature and humidity. Bolted joints play important roles in maintaining structural integrity since their failure could lead to a catastrophic result. Nevertheless, bolts have often been considered one of the most neglected mechanical elements in engineering design of machines and structures. An appropriately applied preload to a bolt ensures a sufficient clamping force to prevent malfunctions such as self-loosening, joint slip, joint separation, and fatigue failure of the bolt, but it is usually difficult to accurately control the fastening behavior of bolted joints due to the complex shape of bolts and high preload sensitivity which varies greatly even with very small angle change [1–3]. To improve the reliability and durability of machine parts, bolts must be properly tightened to pre-specified values of preload. Furthermore, structural bolted joints are increasingly garnering attention in the automotive industry because of failure of bolts under harsh conditions and noise problems such as buzz, squeak and rattle due to insufficient preload [4]. However, tens or hundreds (or even thousands) of bolts are

used in one machine part and it is difficult to directly measure the accurate preload of bolts during fastening process [5,6].

Bolt-tightening methods in real engineering practices are classified into two types based on whether the bolt tightening is performed in the elastic or plastic region. The most commonly used and easiest tightening method in the elastic region is the torque-control method. Here, a preload can be easily predicted from the applied torque and coefficients of friction (COF). However, it is difficult to measure the accurate COF, and the variation of COF causes the variation of the preload, resulting in a poor estimation of preload. Even if the entire tightening process is precisely performed, a preload variation of $\pm$30% is expected when the torque-control method is used in the elastic region [7,8]. Determination of the preload by measuring the turn angle can be an alternative, known as the angle-control method. This method is relatively insensitive to COF and gives more accurate results than the torque-control method as long as the relative angle between a bolt and nut is precisely measured, which is not easy to implement in real engineering practices [9,10].

For the bolt tightening over the yield point, the torque plus angle-control method can be adopted, in which a low torque is first exerted for snugging followed by turn of angle up to a prescribed value. Its variation of preload mainly depends on the variation of bolt's yield strength, so this method has a lesser preload variation than either torque control method or angle control method [11]. Tightening over the yield point can increase the resistance of self-loosening and fatigue failures by applying a sufficient preload to the bolt; however, the risk of bolt rupture during tightening exists due to over-tightening [12,13]. Another alternative is the torque-gradient method where torque, angle, and their gradient are continuously monitored. The tightening process is completed by considering all the three values, especially the gradient. However, this method requires an expensive tool system as well as a longer process time, and there is also the possibility of the risk of over-tightening [12,14].

In contrast to torque-related methods, the elongation control methods such as applications of strain gages, fiber Bragg-grating (FBG) sensors, ultrasonic wave, and vision analysis can offer much more precise and reliable predictions. However, they usually are not cost-effective since special preparations for bolts are required before tightening. Strain gages need to be mounted on a bolt using a special adhesive, so they are not reusable. Optical FBG sensors might be reusable, but a hole penetrating through a bolt is necessary for an optical fiber and the sensor should be glued to the bolt using an adhesive [15–17]. For measuring the preload of a bolt using an ultrasonic wave based on the acoustoelastic effect, there are some conditions required to ensure accuracy: the grip length has to be sufficiently large to minimize errors [18]; the bolt material should be isotropic, and both end surfaces of the bolt need to be flat and parallel [19]; in addition, the measurement accuracy is not ensured under the external vibration, which can change the position of ultrasonic transducer [20,21]. An electromagnetic transducer for measurement of a bolt preload also requires head-to-end parallelism [22]. For an optical inspection technology via automatic digital image correlation to measure the axial strain of a bolt, bolts should be externally exposed to be captured by a vision system [23].

Currently, there has been a continuous demand from industries for a more practical way for estimating the preload so as to apply the monitoring system to production lines. Particularly, for the automobile industry, the development of such application is still challenging. This technology should exhibit the following major attributes: accuracy, low cost, simplicity, and effectiveness. However, insofar no technology has been able to satisfy all of the above-mentioned requirements [24,25]. Furthermore, most of the works have focused on monitoring the structural integrity of the bolted joints during machine operation after a tightening step such as monitoring the fatigue crack of the joints and detecting contact status between the clamped parts, although up to 90% of the failures originate from an inappropriate preload application in the initial tightening process [26,27].

This work aims at introducing a simple and inexpensive linear variable differential transformer (LVDT)-based in situ preload monitoring system (L-PMS). Instead of measuring the elongation of a bolt, the distance between the end surfaces of a bolt and nut was measured using a specially-designed L-PMS, which could be easily mounted onto and dismounted from the bolted joint. Finite element analysis

(FEA) was first performed to evaluate the stiffness of the bolt and clamped part. The developed L-PMS was then tested for tightening bolts and nuts of a truck wheel assembly, in order to find a correlation between the output of the L-PMS and the preload. For more accurate estimation by eliminating the snugging effect, the variation of resistance around a nut bearing surface during the snugging process was also investigated. Finally, preloads predicted by the L-PMS were compared to those measured by a washer-type load cell. The proposed L-PMS was simple, effective and inexpensive, yet showed acceptable accuracy. It would be expected that L-PMS could be utilized in measuring the bolt preload during tightening in a production line.

2. Concept of L-PMS

A typical bolted joint is shown in Figure 1a. If torque is exerted to a bolt, the bolt experiences an elongation and thus a preload (F_p), while the clamped parts are compressed. At the same time, distance between the end surfaces of both the bolt and nut, D_{bn}, is varied. It should be noted that D_{bn} depends on the axial displacements of bolt and clamped parts, Δ_b and Δ_c. Under the assumption that all parts are appropriately snugged, Δ_b and Δ_c are determined in terms of the stiffness and the preload as shown in the following equations [28].

$$\Delta_b = \frac{F_p}{k_b} = \delta_b F_p \tag{1}$$

$$\Delta_c = \frac{F_p}{k_c} = \delta_c F_p \tag{2}$$

where k_b and k_c are the stiffness of bolt and clamped parts, respectively, and δ_b and δ_c denote the corresponding compliances. Since D_{bn} is the sum of Δ_b and Δ_c,

$$D_{bn} = \Delta_b + \Delta_c = F_p\left(\frac{1}{k_b} + \frac{1}{k_c}\right) = F_p(\delta_b + \delta_c) \tag{3}$$

D_{bn} is a linear function of F_p if the stiffness (or compliances) of the bolt and clamped parts are constant [9,10]. This means that the preload can be estimated by measuring the distance variation between the end surfaces of bolt and nut. The proposed L-PMS uses this principle to measure the bolt preload, and a simple concept design of L-PMS is shown in Figure 1b. This structure allows L-PMS to easily measure D_{bn} during tightening of a nut without any interference with a torque wrench.

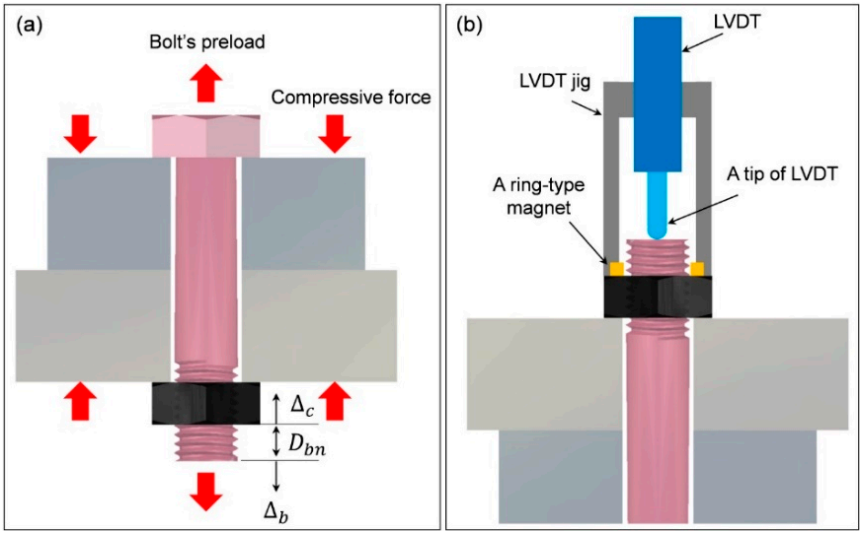

Figure 1. Schematic diagrams of (**a**) the common bolted joint and (**b**) the concept of L-PMS.

3. Materials and Methods

3.1. Materials

For experiments and computational analyses, all the parts of a truck wheel were prepared. Figure 2a shows a hub bolt (M18, strength grade 10.9) with a fine pitch (1.5 mm) and a wheel nut, which are based on the specifications of the international organization for standardization (ISO) [29]. A hub assembly and a wheel were shown in Figure 2b,c, respectively. A total of six hub bolts with serrations in their shanks were press-fitted to the hub assembly, so the bolts did not move during fastening. The hub assembly was then fastened to the wheel using six wheel nuts. Detailed specifications of the bolt used in this study are listed in Table 1. Note that the nominal tensile yield force, F_Y, under pure tension is as high as 203 kN.

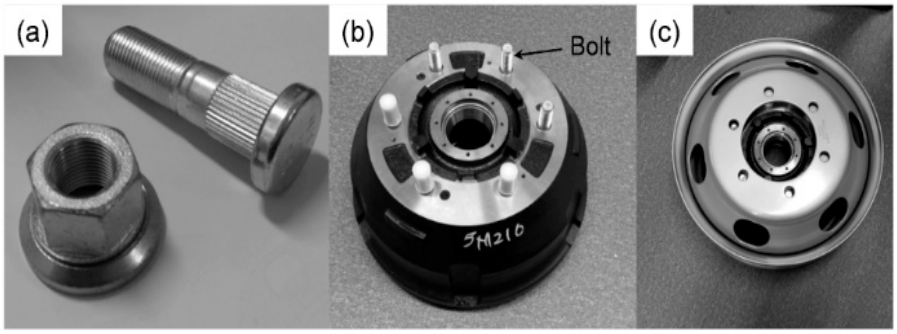

Figure 2. Materials used in this work: (**a**) a bolt and nut, (**b**) a hub assembly with six bolts, and (**c**) a truck wheel placed onto the hub assembly in (**b**).

Table 1. Specifications of the bolt used in this work.

Parameters	Value
Major diameter (d, mm)	18
Pitch (P, mm)	1.5
Yield strength (σ_{Ymin}, MPa)	940
Nominal yield force (F_Y, kN)	203

3.2. Preparation of L-PMS

In order to measure D_{bn}, the L-PMS that consists of only three parts was manufactured: LVDT (S3C, Honeywell Co. Minneapolis, MN, USA), a customized tube-type steel jig, and a ring-type magnet (see Figure 3a,b). LVDT was inserted into the jig and held using four small bolts, and the ring-type magnet played a role in fixing the LVDT jig to the top surface of nut (Figure 3c). The L-PMS could be easily mounted onto and dismounted from a nut by using the ring-type magnet. A disk-type magnet was also mounted on the end surface of the bolt (the inset of Figure 3c) in order to readily obtain a uniform, flat surface from somewhat irregular bolt end surfaces, not conducting time-consuming machining process. Before starting measurement, the tip of LVDT of the L-PMS initially touched the top surface of a disk-type magnet to set the zero point.

With this simple structure for L-PMS, it is possible to easily measure the variation in distance, D_{bn}, between the end surfaces of bolt and nut while fastening the nut to produce the bolt preload. This configuration offers several advantages: (1) the proposed L-PMS is low-cost with a simple structure, (2) the measurement process, from preparation to results, is simple and easy to conduct, (3) it can be used for in-situ monitoring of the bolt preload in a production line, and (4) expensive or complex signal processing is not necessary. A commercial, cheap data acquisition (DAQ) device with a 16-bit resolution is sufficient for measuring the output voltage variation.

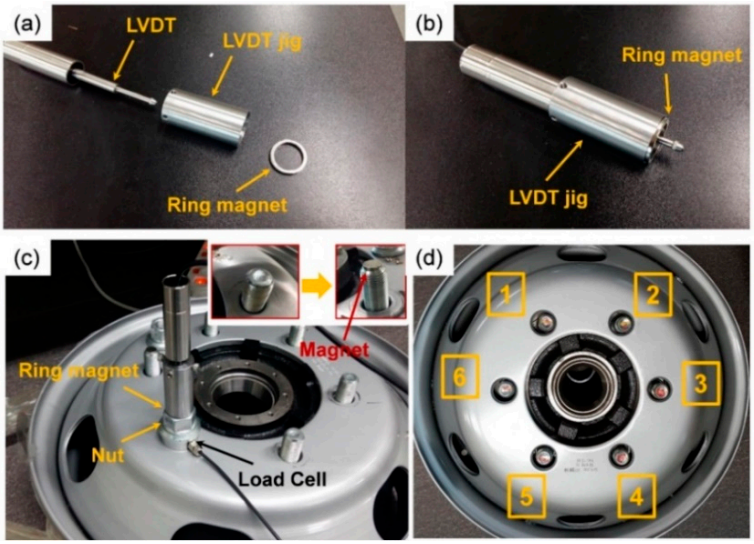

Figure 3. (**a**) Components of the L-PMS: LVDT, customized jig, and ring magnet, (**b**) assembled L-PMS, (**c**) experimental setup, and (**d**) bolt numbering.

3.3. Experimental Details

A total of six identical bolts were connected to the hub assembly, and each bolt was numbered from one to six for the convenience of experiments (Figure 3d). In order to directly measure the actual preload of a bolt, a washer-type load cell (1-KMR/300 kN, HBM Co., Darmstadt, Germany) was placed between the clamped part and nut as shown in Figure 3c. The preload measured by the load cell was correlated with D_{bn} measured by the L-PMS.

As shown in Figure 4, all the data were obtained through a peripheral component interconnect extensions for instrumentation (PXI) system (PXIe-1082, National Instruments Co., Austin, TX, USA) equipped with two DAQ boards (NI-9219 and PXIe-4330, National Instruments Co.) for simultaneously measuring both the displacement from LVDT and the preload from washer-type load cell. A real-time DAQ program was implemented using LabVIEW to record all the data during fastening process. The sampling rate was set to 50 Hz for all the experiments in this study. A manual digital torque wrench (Torcotronic 350, Gedore Co., Remscheid, Germany) was also used to measure the applied torque while tightening the nut. It should be noted that the largest torque that could be manually applied was about 200 N·m, and most experiments were conducted under a torque of 150 N·m. When conducting experiment with one bolt, the other bolts were preliminarily tightened by exerting a relatively low torque of 20 N·m to avoid unnecessary interaction between bolts. The actual preload and D_{bn} were recorded at the same time during the tightening experiments.

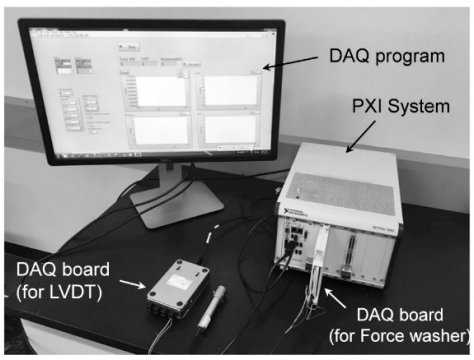

Figure 4. DAQ system for measuring both the displacement from LVDT and the preload from a washer-type load cell.

4. Results and Discussion

4.1. L-PMS Test

Before conducting the experiments with L-PMS, the relationship between the external torque and the bolt preload for the wheel assembly was first investigated. Figure 5 presents the variations in the bolt preload with the externally applied torque. The preload and the torque were measured by a washer-type load cell and a manual digital torque wrench, respectively. The preload tended to be linearly proportional to the torque, but it was in the range of ~25 to ~50 kN under the same torque of 100 N·m, resulting in the preload variation of ±33%. This result shows a typical example of torque-control method. Since only controlling the torque inherently gives a large scatter in the resulting preload, an alternative way is necessary to simply measure the preload in production line.

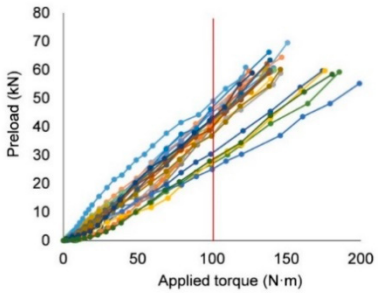

Figure 5. Relationship between externally applied torques and measured preloads.

The L-PMS suggested in this work could be an alternative for measuring the preload with less scatter. Three sets of experiments were conducted for each bolt. The plot in Figure 6a exhibits the relationship between D_{bn} from the L-PMS and the preload from a washer-type load cell. The distance D_{bn} was plotted as a function of the actual preload until reaching 60 kN. It can be seen that there are two different regions, A and B, depending on whether whole parts are fully snugged or not. Such phenomena are not only observed in this study but also in other works. The correlation between displacement of bolted joint and external force is changed before and after the snug point [7,30,31]. The deviation in Region B is generally caused by an initial tolerance between the clamped parts or between the clamped part and nut. If there is such a tolerance, D_{bn} would significantly increase even with a small increase in the preload. D_{bn} exhibits a linear relationship with the preload after all the clamping components are completely snugged. Various logarithm-shaped nonlinear curves were observed before reaching nearly the preload of 30 kN, whereas D_{bn} linearly increased with respect to the preload after 30 kN. Therefore, when the snug point is defined as the point where the linear relationship between D_{bn} and preload just begins, the minimum requirement of snug force was first assumed to be ~30 kN for the whole joint system used in this work. In Figure 6a, it may look linear over the preload of ~15 kN; however, there was a small amount of nonlinearity—the slope (sensitivity) continuously changes—within the range from 10 to 30 kN even though the graph looks linear.

Region A showed a highly linear relationship between D_{bn} and the preload, so Region A was firstly analyzed. The slopes of lines after 30 kN preload were calculated using the least square regression to estimate the sensitivities, and a total of 18 sensitivities were obtained from six bolts and nuts. Figure 6b shows the estimated sensitivities with respect to the bolt number. The sensitivity values were similar for each bolt and nut, and there was a relatively small scatter in them. This is because each bolt was not affected by neighboring bolts during fastening process. Figure 6c shows a histogram for all the sensitivities, which looks like a normal distribution. The averaged sensitivity of all the bolts was 0.662 kN/μm and the standard deviation was 0.024 kN/μm.

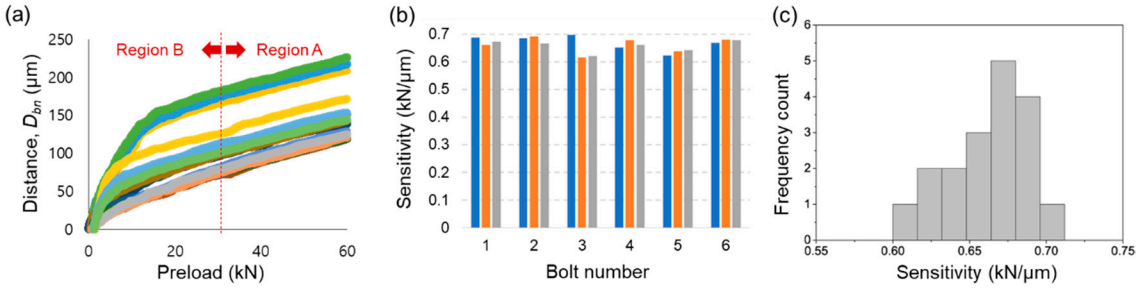

Figure 6. Experimental results: (**a**) variation of distance as a function of preload, (**b**) comparison of the sensitivity of L-PMS from the region A for each bolt (the same color corresponds to the same set of test), and (**c**) histogram for the sensitivities from all the bolts.

The effect of flatness of the bolt's end surface on the reliability of L-PMS was also investigated by detaching the disk-type magnet from the bolt. In this experiment, the bolts were tested as received without any additional processing, and thus their end surfaces were not perfectly flat. When the disk-type magnet was not used, the sensitivity had the average value of 0.619 kN/μm and the standard deviation of 0.047 kN/μm. The averaged sensitivity became lower and the standard deviation was doubled without the disk-type magnet mounted. In the L-PMS, the tip of LVDT initially touches the end surface of bolt, and it also rotates by turning of nut during tightening. An error occurs if the two rotational axes of LVDT and nut are misaligned and the bolt's end surface is not flat. More errors could be produced by the rougher end surface of bolt. It should be noted that the error was reduced by using the disk-type magnet with a flat surface. The tip of LVDT with a larger radius of curvature might help further reduce the effect of the roughness of bolt's end surface.

The variation of D_{bn} from L-PMS was additionally checked by repeated mounting and dismounting as shown in Figure 7. A bolt was tightened up to the preload of 60 kN, and the corresponding D_{bn} was initially measured to 234.97 μm. With the preload fixed to 60 kN, the L-PMS was dismounted from a nut and mounted again several times. The averaged D_{bn} was 234.79 μm, 235.34 μm, 235.33 μm and 235.22 μm in sequence (Figure 7). The standard deviation was 0.27 μm, so the corresponding variation of the preload would be estimated to 0.18 kN considering the sensitivity of 0.662 kN/μm. Therefore, L-PMS could be used not only to measure the preload during fastening process but also to monitor the preload variation in operation.

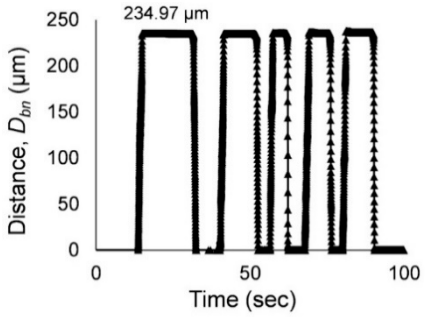

Figure 7. Variation of D_{bn} after mounting and dismounting L-PMS.

4.2. Prediction of Sensitivity from FEA

As emphasized in Equation (3), the stiffness determined by materials and structure is a key factor for the sensitivity of L-PMS, which means that the sensitivity of L-PMS is different depending on a bolt and joint structure used. It is inefficient to find the sensitivity of many different types of bolts and joints only through an experiment in terms of time, cost and applicability. In previous studies, it has been demonstrated that FEA can be used to predict the stiffness of bolt and joint structure directly from the joint geometry and material properties, and the predicted value of stiffness using FEA shows

a good agreement with the actual stiffness [32,33]. Thus, FEA was performed using a commercial FE software ANSYS to predict the stiffness of both the bolt and clamped parts. Analysis models of the bolt and the clamped parts are shown in Figure 8a,b, respectively. Since the bolt and clamped parts were fabricated from structural steel, they were modeled using an isotropic material with the elastic modulus of 205 GPa [34]. For the bolt model, a tetrahedral volume mesh was generated, and the number of elements was 154,247. The head region (serration region) was fixed because the bolt was embedded in a hub assembly via press fitting. An axial tensile force of 1 kN was applied on the end surface of bolt in the normal direction so that the bolt experiences pure tension. For the clamped part model, a one-sixth portion was analyzed due to its cyclic symmetry nature, and the number of elements was 153,200. The axial compressive force of 1 kN was applied on the nut bearing surface in the normal direction, while the bolt head bearing surface was fixed. All contact regions between the wheel and hub assembly were assumed to be bonded because friction between wheel and hub has little effect on the stiffness in pure compression state [35,36].

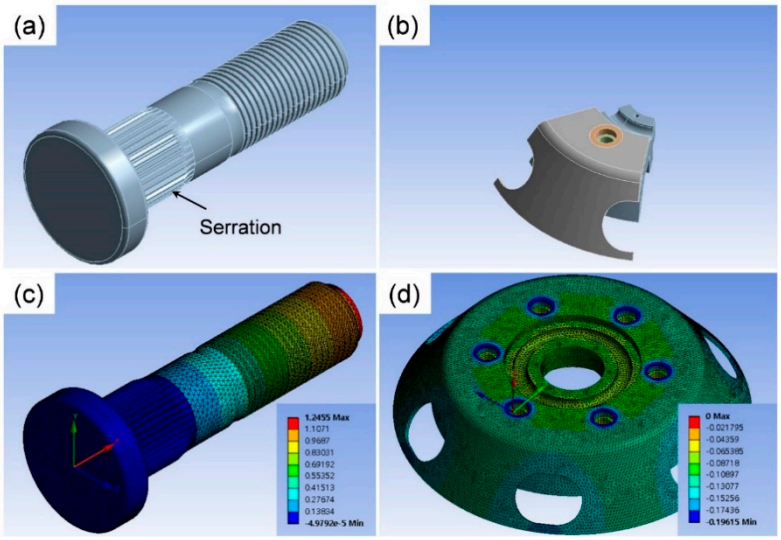

Figure 8. (**a**) Analysis model for the bolt, (**b**) one-sixth analysis model for the clamped parts, (**c**) axial deformation of the bolt under 1 kN tensile force, and (**d**) axial deformation of the clamped parts under 1 kN compressive force. Unit for (**c**) and (**d**) is μm.

Figure 8c,d illustrate the axial deformation of the bolt and the clamped parts under the 1 kN axial force, respectively. The absolute displacements of 1.246 μm and 0.197 μm were generated at the bolt's end surface and the nut bearing surface due to 1 kN axial forces, respectively. These displacement values correspond to the compliances of the bolt and clamped parts, and the equivalent stiffness of joint structure, which is the same as the sensitivity of L-PMS, is calculated as the inverse of the sum of compliances. Therefore, from these compliances (1.246 and 0.197 μm/kN), the sensitivity was predicted to be 0.693 kN/μm. The predicted sensitivity (0.693 kN/μm) was slightly higher than the measured one (0.662 kN/μm). Such difference can be attributed to the simplification of the analytical model. Deformation of threads in the bolt and nut was not considered in the analysis, and the frictional contact regions were assumed bonded. Even though there was a slight difference between the predicted and experimentally-obtained sensitivities, the error was only 4.6%, which is regarded as an acceptable value. This means that the sensitivity of L-PMS can be predicted using FEA when L-PMS is applied to a new structure.

4.3. Determination of Snug Force

L-PMS assumes a linear relationship between D_{bn} and the preload, but irregular logarithm-shaped curves (region B) were observed before the snug point as shown in Figure 6a. In the previous section,

the snug force was graphically selected to be 30 kN; however, in order to more accurately measure the preload, the snug point should be correctly defined. A snug torque, which is much lower than the full tightening torque, is commonly applied to approximately determine the snug point, but it still could lead to a large scatter in the preload because it is also a kind of torque-control method greatly affected by the variation in COF. Thus, a new way was suggested to determine the snug point more accurately.

A conductive line was introduced on the surface in the vicinity of the nut bearing area for measuring the resistance variation during fastening process. As shown in Figure 9, carbon paste was screen-printed to fabricate an arc-shaped conductive line on the top surface of wheel outside the nut bearing surface. Screen printing method has been widely used in the field of printed electronics due to its many advantages such as low cost, process simplicity, and pattern durability [37–39]. After fabricating the conductive line, the resistance variation was measured using a hand-held digital multi-meter (DMM, Hioki Co., Nagano, Japan) while simultaneously monitoring the actual preload and D_{bn}. Figure 10a shows the typical example of the resistance change ratio ($\Delta R/R_0$) as a function of D_{bn}, and the corresponding variation of D_{bn} with the preload is plotted in Figure 10b. $\Delta R/R_0$ began to converge at approximately D_{bn} = 112 μm as D_{bn} increased. The corresponding preload was approximately 38 kN at D_{bn} = 112 μm, which was thought to be the snug force. In the same manner, the averaged snug force and the standard deviation were found to be 42.1 kN and 1.4 kN, respectively, from additional experiments. This value was a little higher than the first-assumed snug force of 30 kN from Figure 6a. Note that this measured snug force (42.1 kN) is only 20.7% of the bolt's nominal tensile yield force (F_Y = 203 kN in Table 1).

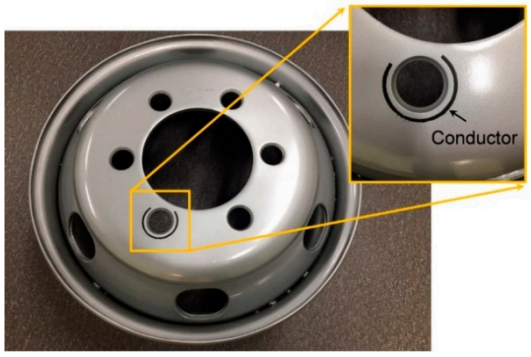

Figure 9. Conductive line screen-printed near the nut bearing surface using carbon paste.

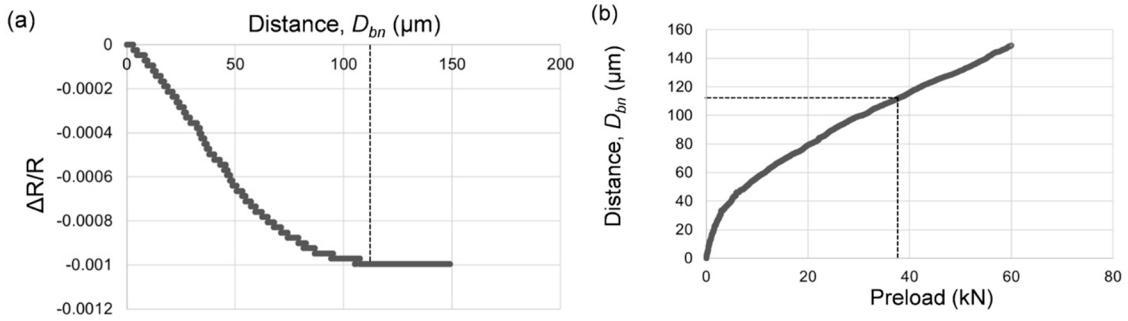

Figure 10. (**a**) Variation in the resistance change ratio with the distance D_{bn} and (**b**) relationship between corresponding preload and the distance D_{bn}.

This correlation among D_{bn}, resistance change, and preload originates from the surface characteristics of the clamped parts. The top surface of the wheel is coated with a thin polymer layer to prevent a contamination and achieve an appropriate COF. In particular, the coating layer has a much lower elastic modulus as compared with steel, so a relatively large deformation of the coating layer occurs near the nut bearing surface by the compressive force due to tightening of the nut, which causes the resistance of the conductive line on the coating layer to be changed. When the

coating layer is fully compressed, the joint reaches to its snug point. At this sung point, the resistance value levels off and begins to remain unchanged; therefore, we can determine the snug point using the measurement of resistance change. It is noteworthy that the snug point where the linear relationship just begins is farther from the origin than it looks as discussed in Section 4.1.

4.4. Estimation of Final Clamping Force

From the combination of the snug force and D_{bn}, the bolt preload can be determined during fastening process. The averaged snug force was measured to 42.1 kN from the previous experiments using the resistance changes, and D_{bn} from the L-PMS was linearly proportional to the preload with a sensitivity of 0.662 kN/μm after the snug point. Therefore, through the combination of resistance measurement and L-PMS, the final bolt preload (F_P) could be estimated as follows:

$$F_P = F_{snug} + \text{sensitivity} \times D_{bn} \quad (4)$$

where F_{snug} = 42.1 kN, sensitivity = 0.662 kN/μm, and D_{bn} is the measured value after the snug point. D_{bn} and $\Delta R/R_0$ should be simultaneously measured to determine the snug point during tightening of the nut. In order to use the value of D_{bn} relative to the snug point, the slope of $\Delta R/R_0$ with respect to D_{bn} was monitored, and D_{bn} was reset to zero just after the slope began to converge.

A total of 12 tests were conducted and compared with the actual preloads independently measured by the washer-type load cell. Figure 11a shows the comparison between the estimated and actual preloads. In the first test, for example, the measured D_{bn} was 31.34 μm, so F_P was estimated to 62.86 kN. On the other hand, the actual preload was measured to 60.04 kN. Compared to the actual preload, the estimated preload showed a 4.6% error. In this manner, all the test results were compared with the actual preloads. The error was found to be within ±6%, which is indeed comparable to other monitoring methods [7,40]. Finally, the relationship between the estimated and actual preloads is presented in the range of ~45 kN to ~60 kN in Figure 11b. The results showed a good linear agreement between the two values.

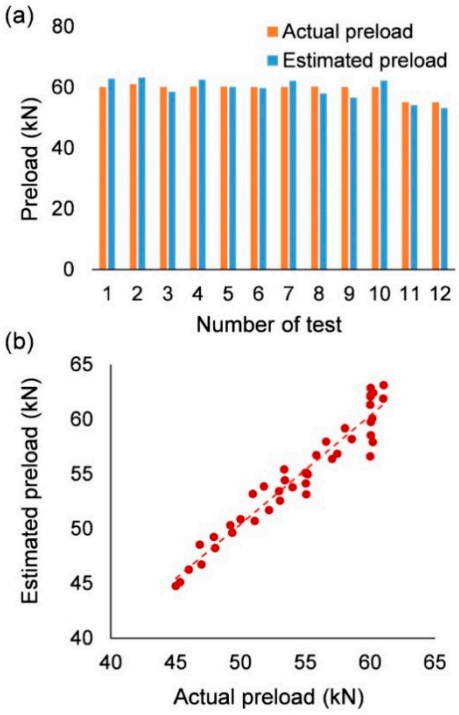

Figure 11. (**a**) Comparison between estimated preloads from the L-PMS and actual preloads measured by the washer-type load cell: (**a**) a bar chart near the actual preload of 60 kN and (**b**) a scatter plot for the actual preloads from 45 kN to 60 kN.

One of the drawbacks of L-PMS is that F_{snug} should be determined prior to using the L-PMS and the preload less than F_{snug} could not be measured. However, as noted, F_{snug} (42.1 kN) is much smaller than the bolt's nominal yield force (F_Y = 203 kN), and the bolt preload is usually set to larger than 70% of F_Y in truck industry; therefore, the proposed L-PMS combined with the resistance measurement could be utilized to estimate the bolt preload especially for a heavy truck production.

5. Conclusions

In summary, an L-PMS was designed and tested to estimate the bolt preload of a truck wheel assembly by measuring the displacement (D_{bn}) between the end surfaces of a bolt and nut. After all the clamping parts were fully snugged, a strong linear relationship between D_{bn} and the preload was observed. The sensitivity of L-PMS was measured to 0.662 $\pm$ 0.024 kN/μm. FEA was also performed to predict the sensitivity, which was in a good agreement with the experimentally-obtained one. In addition, initial nonlinear relationships between D_{bn} and the preload were found before reaching to the snug point, which hinders a reliable estimation of the preload using the L-PMS. In order to more accurately define the snug point, the variation in resistance with the preload was measured using an arc-shaped conductive line printed near the nut bearing surface. The snug point was defined with help of tracking the slope of resistance change ratio, and the snug force of the truck wheel assembly used in this work was estimated to 20.7% of the nominal yield force. By comparing the estimated preload from L-PMS combined with the resistance measurement to the actual preload measured by a washer-type load cell, it was found that the suggested L-PMS showed an error of $\pm$6% and a good linear relationship. The concept of measuring the bolt preload proposed in this work has many advantages in terms of its simplicity, low cost, and reliability, so it could be utilized for monitoring the bolt preloads in the automotive industry.

Author Contributions: S.J. and J.H.O. conceptualized and designed the experiments and analyses; S.J., J.N. and S.L. conducted the experiments; J.N. performed the analyses; S.J., J.N. and J.H.O. analyzed the experimental and analytical data; S.J., J.N. and J.H.O. wrote the paper.

Funding: This work was supported by Hyundai Motor Company. It was also supported by the Korea Institute of Energy Technology Evaluation and Planning (KETEP), grant funded by the Korea Government Ministry of Trade, Industry and Energy (MOTIE) (No. 20174010201310).

Conflicts of Interest: The authors declare no conflict of interest.

References

1. Kim, J.; Yoon, J.C.; Kang, B.S. Finite element analysis and modeling of structure with bolted joints. *Appl. Math. Model.* **2007**, *31*, 895–911. [CrossRef]
2. Kwon, Y.D.; Kwon, H.W.; Hwangbo, J.H.; Jang, S.H. Finite element modeling for static and dynamic analysis of structures with bolted joint. *Key Eng. Mater.* **2006**, *306–308*, 547–552. [CrossRef]
3. Ganeshmurthy, S.; Nassar, S.A. Finite Element Simulation of Process Control for Bolt Tightening in Joints with Nonparallel Contact. *J. Manuf. Sci. Eng. ASME* **2014**, *136*, 021018. [CrossRef]
4. Trapp, M.; Chen, F. *Automotive Buzz, Squeak and Rattle: Mechanisms, Analysis, Evaluation and Prevention*, 1st ed.; Butterworth-Heinemann: Oxford, UK, 2012.
5. Abid, M.; Khan, Y.M. The effect of bolt tightening methods and sequence on the performance of gasketed bolted flange joint assembly. *Struct. Eng. Mech.* **2013**, *46*, 843–852. [CrossRef]
6. Abid, M.; Nash, D.H. Structural strength: Gasketed vs non-gasketed flange joint under bolt up and operating condition. *Int. J. Solids Struct.* **2006**, *43*, 4616–4629. [CrossRef]
7. Toth, G.R. Torque and angle controlled tightening over the yield point of a screw-based on Monte-Carlo simulations. *J. Mech. Des.* **2004**, *126*, 729–736. [CrossRef]
8. Croccolo, D.; de Agostinis, M.; Vincenzi, N. A contribution to the selection and calculation of screws in high duty bolted joints. *Int. J. Press. Vessels Pip.* **2012**, *96–97*, 38–48. [CrossRef]
9. Bickford, J.H.; Nassar, S. *Handbook of Bolts and Bolted Joints*; M. Dekker: New York, NY, USA, 1998.
10. Bickford, J.H. *Introduction to the Design and Behavior of Bolted Joints*, 4th ed.; CRC Press: Boca Raton, CA, USA, 2008.

11. Monaghan, J.M. The Influence of Lubrication on the Design of Yield Tightened Joints. *J. Strain Anal. Eng. Des.* **1991**, *26*, 123–132. [CrossRef]
12. Junker, G.H.; Wallace, P.W. The Bolted Joint—Economy of Design through Improved Analysis and Assembly Methods. *Proc. Inst. Mech. Eng. B* **1984**, *198*, 255–266. [CrossRef]
13. Bickford, J.H. *An Introduction to the Design and Behavior of Bolted Joints*, 2nd ed.; M. Dekker: New York, NY, USA, 1990.
14. Boys, J.T.; Tambini, A. Tightening Methods for Fasteners. *Engineering* **1981**, *221*, R1–R4.
15. Khomenko, A.; Koricho, E.G.; Haq, M.; Cloud, G.L. Bolt tension monitoring with reusable fiber Bragg-grating sensors. *J. Strain Anal. Eng. Des.* **2016**, *51*, 101–108. [CrossRef]
16. Hackney, D.; Peters, K. Damage Identification After Impact in Sandwich Composites Through Embedded Fiber Bragg Sensors. *J. Intell. Mater. Syst. Struct.* **2011**, *22*, 1305–1316. [CrossRef]
17. Pereira, G.; Frias, C.; Faria, H.; Frazao, O.; Marques, A.T. On the improvement of strain measurements with FBG sensors embedded in unidirectional composites. *Polym. Test.* **2013**, *32*, 99–105. [CrossRef]
18. Nassar, S.A.; Veeram, A.B. Ultrasonic control of fastener tightening using varying wave speed. *J. Press. Vessel Trans. ASME* **2006**, *128*, 427–432. [CrossRef]
19. Chaki, S.; Corneloup, G.; Lillamand, I.; Walaszek, H. Combination of longitudinal and transverse ultrasonic waves for in situ control of the tightening of bolts. *J. Press. Vessel Technol. ASME* **2007**, *129*, 383–390. [CrossRef]
20. Persson, E.; Roloff, A. Ultrasonic tightening control of a screw joint: A comparison of the clamp force accuracy from different tightening methods. *Proc. Inst. Mech. Eng. C-J. Mech.* **2016**, *230*, 2595–2602. [CrossRef]
21. Joshi, S.G.; Pathare, R.G. Ultrasonic Instrument for Measuring Bolt Stress. *Ultrasonics* **1984**, *22*, 270–274. [CrossRef]
22. Hirao, M.; Ogi, H.; Yasui, H. Contactless measurement of bolt axial stress using a shear-wave electromagnetic acoustic transducer. *NDT E Int.* **2001**, *34*, 179–183. [CrossRef]
23. Huang, Y.H.; Liu, L.; Yeung, T.W.; Hung, Y.Y. Real-time monitoring of clamping force of a bolted joint by use of automatic digital image correlation. *Opt. Laser Technol.* **2009**, *41*, 408–414. [CrossRef]
24. Parvasi, S.M.; Ho, S.C.M.; Kong, Q.Z.; Mousavi, R.; Song, G. Real time bolt preload monitoring using piezoceramic transducers and time reversal technique-a numerical study with experimental verification. *Smart Mater. Struct.* **2016**, *25*, 085015. [CrossRef]
25. Wang, T.; Song, G.B.; Wang, Z.G.; Li, R.Y. Proof-of-concept study of monitoring bolt connection status using a piezoelectric based active sensing method. *Smart Mater. Struct.* **2013**, *22*, 087001. [CrossRef]
26. Rakow, A.; Chang, F.K. A structural health monitoring fastener for tracking fatigue crack growth in bolted metallic joints. *Struct. Health Monit.* **2012**, *11*, 253–267. [CrossRef]
27. Wang, T.; Liu, S.P.; Shao, J.H.; Li, Y.R. Health monitoring of bolted joints using the time reversal method and piezoelectric transducers. *Smart Mater. Struct.* **2016**, *25*, 025010.
28. Barrett, R.T. *Fastener Design Manual*; National Aeronautics and Space Administration, Office of Management, Scientific and Technical Information Devision: Washington, DC, USA, 1990.
29. *ISO 292 International Organization for Standardization for General Purpose Metric Screw Threads—Selected Sizes for Screw, Bolts and Nut*; ISO: Geneva, Switzerland, 1998.
30. Faella, C.; Piluso, V.; Rizzano, G. Experimental analysis of bolted connections: Snug versus preloaded bolts. *J. Struct. Eng.-ASCE* **1998**, *124*, 765–774. [CrossRef]
31. Toth, G.R. Controlled tightening over the yield point of a screw: Based on Taylor's series expansions. *J. Press. Vessel-Technol. ASME* **2003**, *125*, 460–466. [CrossRef]
32. Wileman, J.; Choudhury, M.; Green, I. Computation of Member Stiffness in Bolted Connections. *J. Mech. Des.* **1991**, *133*, 432–437. [CrossRef]
33. Nassar, S.A.; Abboud, A. An Improved Stiffness Model for Bolted Joints. *J. Mech. Des.* **2009**, *131*, 11. [CrossRef]
34. Society of Automotive Engineers (SAE). *Ferrous Materials Standards Manual*; Society of Automotive Engineers: Warrendle, PA, USA, 1999.
35. Musto, J.C.; Konkle, N.R. Computation of Member Stiffness in the Design of Bolted Joints. *J. Mech. Des.* **2005**, *128*, 1357–1360. [CrossRef]
36. Huda, F.; Kajiwara, I.; Hoseya, N.; Kawamura, S. Bolt loosening analysis and diagnosis by non-contact laser excitation vibration tests. *Mech. Syst. Signal Process.* **2013**, *40*, 589–604. [CrossRef]

37. Dungchai, W.; Chailapakul, O.; Henry, C.S. A low-cost, simple, and rapid fabrication method for paper-based microfluidics using wax screen-printing. *Analyst* **2011**, *136*, 77–82. [CrossRef] [PubMed]
38. Erath, D.; Filipovic, A.; Retzlaff, M.; Goetz, A.K.; Clement, F.; Biro, D.; Preu, R. Advanced screen printing technique for high definition front side metallization of crystalline silicon solar cells. *Sol. Energy Mater. Sol. Cells* **2010**, *94*, 57–61. [CrossRef]
39. Jost, K.; Stenger, D.; Perez, C.R.; Mcdonough, J.K.; Lian, K.; Gogotsi, Y.; Dion, G. Knitted and screen printed carbon-fiber supercapacitors for applications in wearable electronics. *Energy Environ. Sci.* **2013**, *6*, 2698–2705. [CrossRef]
40. Oberg, E.; Jones, F.D. *Machinery's Handbook*, 27th ed.; Industrial Press: New York, NY, USA, 2004.